Acta Crystallographica Section D
**Biological Crystallography**
ISSN 0907-4449

# Generation of noble-gas binding sites for crystallographic phasing using site-directed mutagenesis

**Michael L. Quillin and Brian W. Matthews***

Institute of Molecular Biology, Howard Hughes Medical Institute and Department of Physics, 1229 University of Oregon, Eugene, OR 97403-1229, USA

Correspondence e-mail: brian@uoxray.uoregon.edu

Received 22 June 2001
Accepted 25 October 2001

In recent years, the use of noble-gas complexes for the *de novo* phasing of protein structures has proven to be a useful alternative to selenomethionine and more traditional derivatives, largely owing to improvements in methods for incorporating noble gases within protein crystals. Advantages of noble-gas derivatives include a high degree of isomorphism when using xenon for multiple isomorphous replacement (MIR) and an easily accessible absorption edge when using krypton for multiwavelength anomalous dispersion (MAD) phasing. One problem with this approach is that not all proteins contain cavities which bind noble gases. Even in proteins which do bind noble gases, the resulting derivative may not be sufficient for phasing. Using T4 lysozyme as an example, it is illustrated how this limitation might be overcome by using 'large-to-small' mutations to introduce potential noble-gas binding sites. Wild-type T4 lysozyme contains a single xenon-binding site. By truncating leucine and phenylalanine residues to alanine, it is possible to generate additional noble-gas binding sites within the core of the protein. Combining rotating-anode data from xenon complexes of wild-type and mutant lysozymes yields MIR phases which compare favorably with those determined from a selenomethionine MAD experiment conducted at a synchrotron. Experience with T4 lysozyme suggests that a leucine-to-alanine substitution made at random in a protein of unknown structure has about a 30% chance of providing a useful derivative. This procedure holds promise for the determination of unknown protein structures, especially when selenomethionine-containing protein is not available or when access to a synchrotron is limited.

## 1. Introduction

The combination of multiwavelength anomalous dispersion (MAD) phasing with methods for incorporating selenomethionine into proteins has revolutionized protein crystallography (Hendrickson & Ogata, 1997). Conditions for producing selenomethionine-substituted proteins in *Escherichia coli* are now well established (Hendrickson *et al.*, 1990; Doublie, 1997). Unfortunately, many eukaryotic proteins cannot be overexpressed in prokaryotic systems owing to requirements of post-translational modification (*e.g.* glycosylation and disulfide-bond formation) for proper folding. Although selenomethionine incorporation has recently been achieved in insect (Chen & Bahl, 1991; Bellizzi *et al.*, 1999; McWhirter *et al.*, 1999) and mammalian cells (Lustbader *et al.*, 1995), the difficulty of optimizing conditions in these eukaryotic systems may prevent this method from becoming routinely applied. Even in proteins in which

**Table 1**
Data-collection statistics for xenon and selenomethionine derivatives.

L99A is the mutant lysozyme with leucine 99 replaced by alanine. L99A SeMet is the same mutant with all five methionines replaced by selenomethionine. L99A/F153A is the double mutant L99A plus F153A.

| Protein | Wavelength (Å) | Resolution (Å) | Measured reflections | Unique reflections | Completeness (%) | $R_{merge}$ (%) |
|---|---|---|---|---|---|---|
| WT* | 1.5418 | 1.9 | 50396 | 16083 | 95.1 | 5.9 |
| WT* in 0.8 MPa Xe | 1.5418 | 2.0 | 41643 | 13227 | 91.0 | 6.0 |
| L99A in 0.8 MPa Xe | 1.5418 | 1.9 | 60389 | 16522 | 96.7 | 5.4 |
| F153A in .08 MPa Xe | 1.5418 | 2.3 | 33143 | 9602 | 97.5 | 9.6 |
| L99A/F153A in 0.8 MPa Xe | 1.5418 | 2.2 | 23164 | 9626 | 86.2 | 6.0 |
| L99A SeMet | 0.9998 (low) | 1.6 | 229460 | 49702 | 98.8 | 4.8 |
| L99A SeMet | 0.9794 (inflection) | 1.6 | 238166 | 50043 | 99.6 | 5.1 |
| L99A SeMet | 0.9792 (peak) | 1.6 | 240518 | 50268 | 99.7 | 5.1 |
| L99A SeMet | 0.9691 (high) | 1.6 | 247238 | 51477 | 99.7 | 4.9 |

selenomethionine can be successfully introduced, the heterogeneity which arises from partial oxidation of selenomethionine residues can reduce the strength of the already weak anomalous signal (Smith & Thompson, 1998; Sharff *et al.*, 2000).

Some alternatives to selenomethionine incorporation include the use of naturally occurring noble-gas binding sites (Vitali *et al.*, 1991; Cohen *et al.*, 2001), the use of halide-binding sites (Dauter *et al.*, 2001; Dauter & Dauter, 2001) and the use of introduced cysteines (Dao-Pin *et al.*, 1987) as well as conventional heavy-atom derivatives.

Here, we propose an alternate method for *de novo* phase determination which relies upon the binding of noble gases within engineered cavities in proteins. By mutating large apolar residues such as leucine and phenylalanine to alanine, one or more noble-gas binding sites may be readily introduced into a protein of interest. The binding sites that result from such 'large-to-small' mutations provide an avenue for obtaining multiple xenon derivatives. It is shown that the quality of the multiple isomorphous replacement (MIR) phases obtained from unfrozen crystals of such xenon complexes on a rotating-anode source is comparable to that of MAD phases derived from frozen selenomethionine-containing crystals at a synchrotron.

## 2. Methods

Crystallization and data collection for xenon complexes of wild-type and mutant lysozymes in the $P3_221$ space group have been described previously (Quillin *et al.*, 2000). (In this work, 'wild type' and 'WT*' refer to the cysteine-free pseudo wild-type protein described by Matsumura & Matthews, 1989.) Briefly, 0.5–1.0 mm crystals were mounted in a quartz capillary pressure cell using the technique described by Schiltz *et al.* (1994). Xenon was introduced into the system through several purge cycles, then maintained at 0.8 MPa for 2 h prior to, as well as during, data collection. Diffraction data for xenon derivatives were measured on an R-AXIS IIC image-plate detector (Molecular Structure Corp., Houston, Texas) using a rotating-anode source with a graphite monochromator. Typically, 40 frames were collected with an oscillation range of 1.5° and an exposure time of 30 min. The crystals were cooled to a temperature of approximately 277 K during data collection in order to minimize radiation damage.

Protein containing selenomethionine was expressed as described previously (Gassner *et al.*, 1999). Crystals of selenomethionine-labeled protein grew under conditions similar to the unlabeled protein. A 0.2 mm crystal of selenomethionine-containing L99A lysozyme was flash-frozen without cryoprotectant in a nitrogen cold-stream at 100 K. After determining inflection and peak wavelengths from a fluorescence scan, a four-wavelength MAD data set was collected at Advanced Light Source beamline 5.021 with a Quantum-4 CCD detector (ADSC, San Diego, California). To optimize the anomalous signal at each wavelength, two sweeps were collected using the inverse-beam method with a wedge size of 20°. Each sweep consisted of 80 frames with an oscillation range of 1.0° and an exposure time of 5 s.

Diffraction data were processed using *DENZO* and *SCALEPACK* (Otwinowski & Minor, 1997). Patterson maps were calculated using the *CCP*4 program suite (Collaborative Computational Project, Number 4, 1994). Heavy-atom parameters were refined and phases were calculated using *SHARP* (de La Fortelle & Bricogne, 1997). Because many of the sites were present in more than one mutant, only five sites were refined for the xenon derivatives, with each mutant being assigned a subset of these five sites. Phase improvement using solvent flattening was performed using the *SOLOMON* (Abrahams & Leslie, 1996) routines distributed with *SHARP*.

## 3. Results

To obtain crystallographic phases using multiple isomorphous replacement (MIR), data were collected from crystals of wild-type, L99A, F153A and L99A/F153A lysozyme in the presence of 0.8 MPa xenon as well as wild-type lysozyme in the absence of xenon (Table 1). These data sets were collected on unfrozen crystals on a rotating-anode source, giving data to 1.9–2.3 Å, and were fairly complete with approximately threefold redundancy. For comparison, a multiwavelength anomalous dispersion (MAD) experiment was conducted on selenomethionine-containing L99A lysozyme. In addition to peak and inflection data sets, both high and low remote data sets were also collected. Because these data sets were collected on a frozen crystal at a synchrotron, the resolution, completeness and redundancy are considerably higher than the data for the xenon derivatives (Table 1).

In isomorphous difference Patterson maps calculated for the xenon derivatives, most sites give rise to peaks that are clearly visible in the $w = 1/3$ Harker section (Fig. 1). The peak

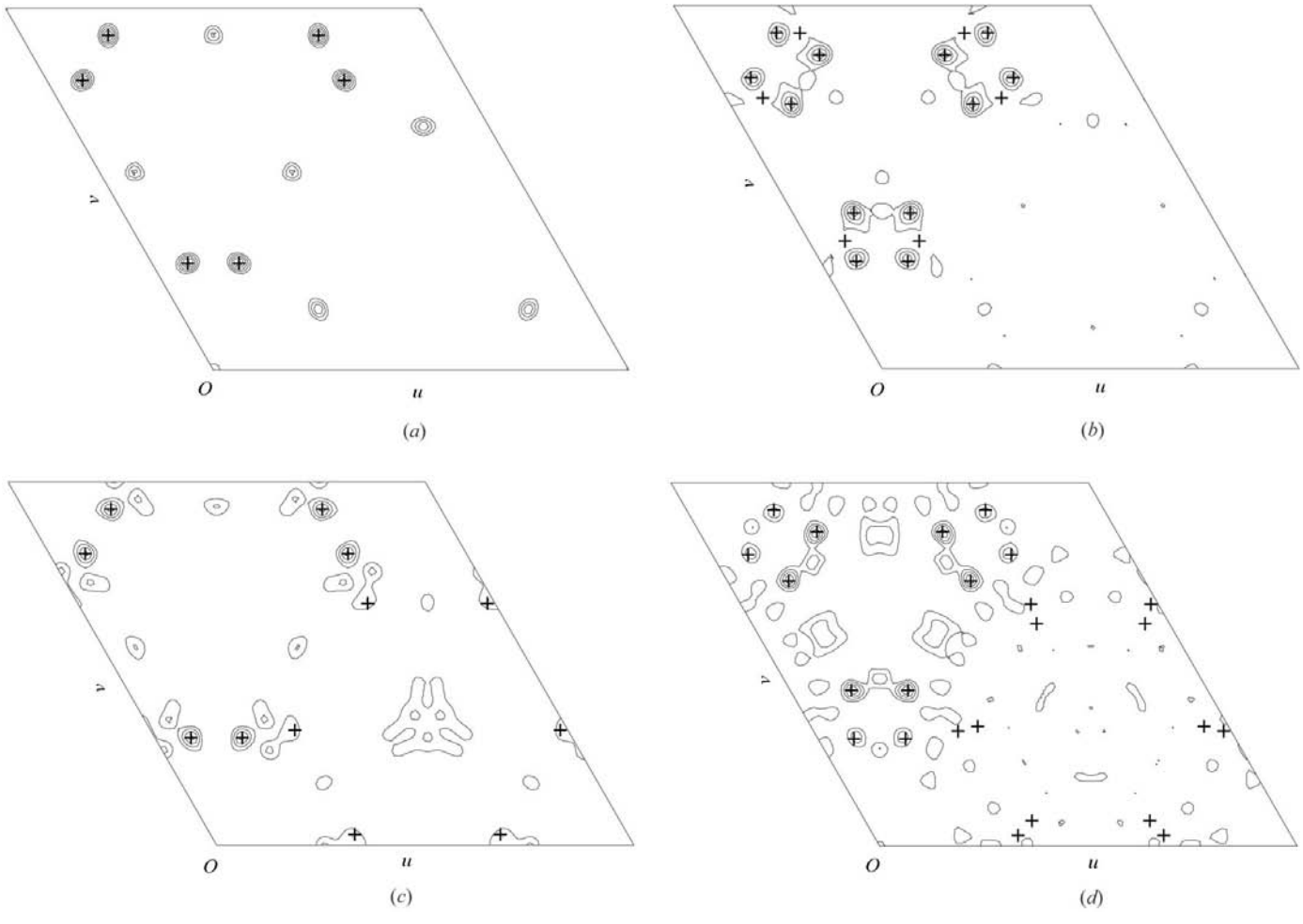


**Figure 1**
Harker sections ($w$ = 1/3) of isomorphous difference Patterson maps for xenon derivatives. In each case, the coefficients are of the form $(F_{\text{protein plus Xe}} - F_{\text{protein}})^2$ and the resolution is 2.5 Å. The crosses show the Harker vectors expected from the refined xenon positions. (*a*) Wild-type lysozyme; contours drawn at increments of $3\sigma$, where $\sigma$ is the root-mean-square density throughout the unit cell. Contours for zero and negative density are omitted. (*b*) Mutant L99A contoured at increments of $2\sigma$. (*c*) Mutant F153A contoured at increments of $2\sigma$. (*d*) Double mutant L99A/F153A contoured at increments of $1\sigma$.

in the wild-type difference Patterson map has a height of $15\sigma$, while in the mutants the strongest peaks are typically 6–$8\sigma$. The weaker sites in these maps were apparent only in residual difference Fourier maps. In the anomalous difference Patterson map for the selenomethionine derivative (Fig. 2), the strongest two peaks have heights of 10 and $5\sigma$, while the remaining three peaks give much weaker signals. As is evident from the figures, the xenon data gave isomorphous difference Patterson maps which were at least as clear as the anomalous difference map obtained from selenomethionine data. Since anomalous signals are typically much weaker than isomorphous differences, this is not strictly speaking a fair comparison. From an experimental standpoint, however, these are the maps that must be interpreted before phases can be obtained.

Maximum-likelihood refinement of the xenon and selenomethionine derivatives using *SHARP* (de La Fortelle & Bricogne, 1997) gave reasonable values for heavy-atom positions, *B* factors and occupancies (Table 2). Sites 1 and 2 had occupancies of approximately 0.5 with *B* factors between 10 and 20 Å$^2$, while sites 3, 4 and 5 were considerably weaker. In

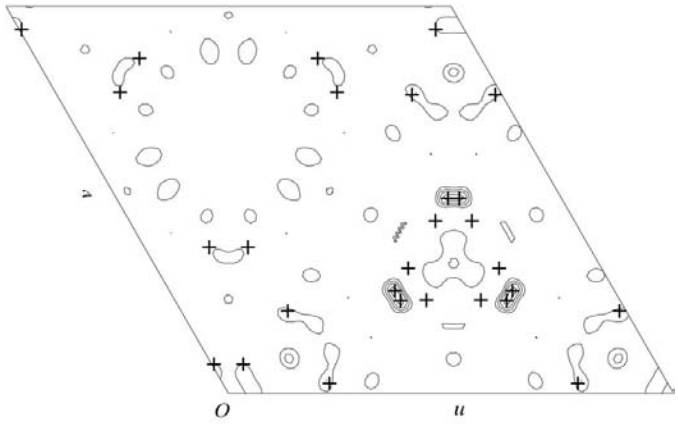


**Figure 2**
Harker section ($w$ = 1/3) of an anomalous difference Patterson map for selenomethionine-containing L99A lysozyme calculated using 'peak' data ($\lambda$ = 0.9792 Å; Table 1). Vectors from refined selenium positions are shown as crosses. The resolution is 2.5 Å and the map is contoured at increments of $1.5\sigma$.

the case of the selenomethionine derivative, the $B$ factors ranged from 10 to 70 Å$^2$ with occupancies between 0.9 and 1.5. Fixing the selenium occupancies at unity gave $B$ factors between 10 and 50 Å$^2$.

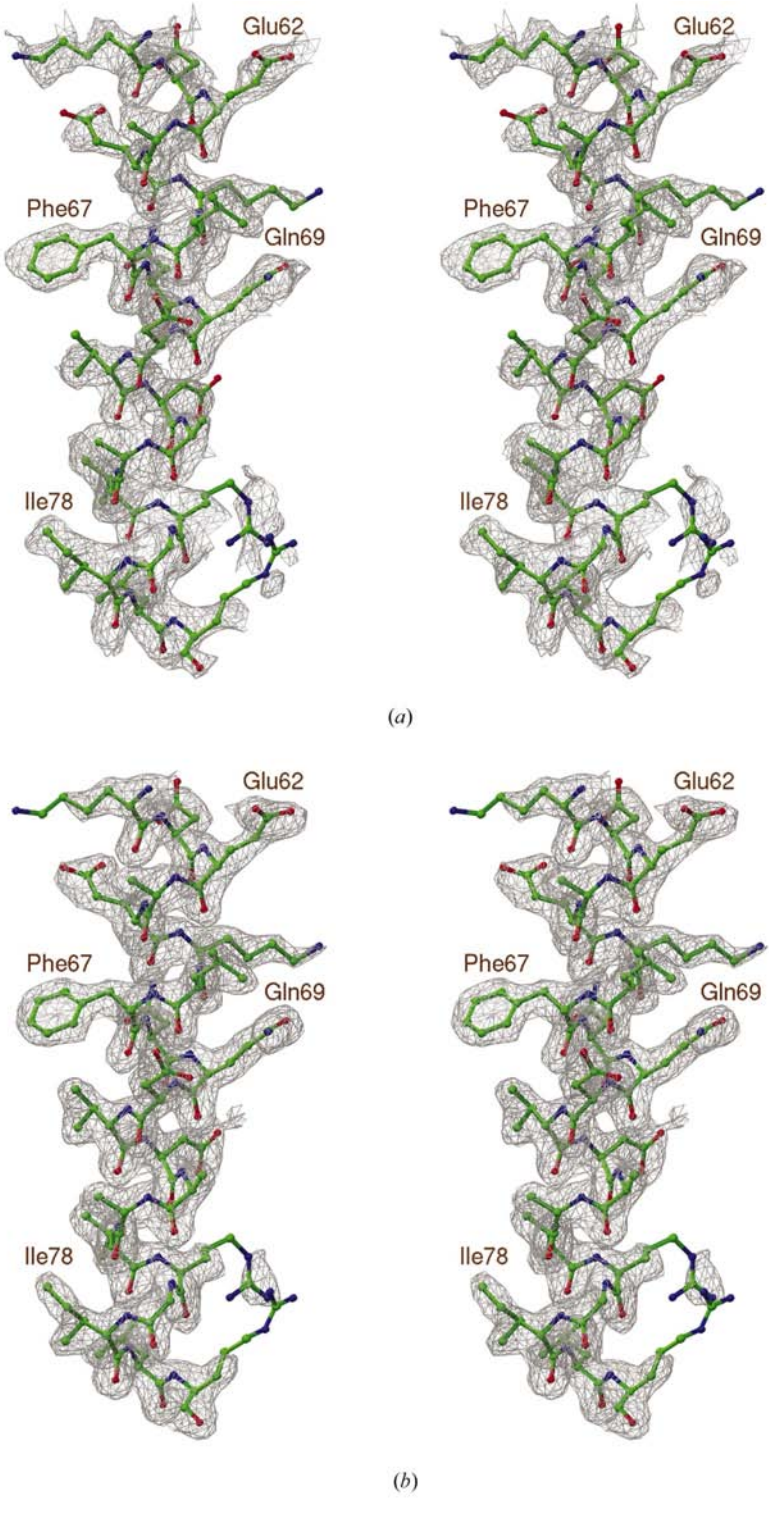


**Figure 3**
Stereoviews of representative electron density calculated using experimental phases from xenon derivatives (*a*) before and (*b*) after solvent flattening. The maps, which are at a resolution of 1.9 Å and contoured at 1.0$\sigma$, depict the central helix (residues 60–80) of lysozyme. Refined coordinates for wild-type lysozyme are superimposed.

As expected, in the case of xenon the best source of phase information came from isomorphous differences, while anomalous differences were more important in phase determination *via* the selenomethionine data. As shown in Table 3, the isomorphous phasing power is greater than 1.5 for each of the xenon derivatives, while the values for the anomalous signal are significantly lower. For the selenomethionine MAD data, the highest values of the phasing power were obtained from the inflection, peak and high remote anomalous data, with values between 4 and 6. Although not as strong as the anomalous signal, the dispersive differences treated as isomorphous differences from the inflection and peak data sets also contributed significantly to the overall phase determination. The figures of merit presented in Table 3 indicate that prior to solvent flattening the phases obtained from the xenon data were poorer than those from the selenomethionine data; however, density modification with *SOLOMON* (Abrahams & Leslie, 1996) improved the figures of merit to greater than 0.9 in both cases.

While the figure of merit and phasing power provide an indication of phase error, the most important measure of phase accuracy lies in the quality of the electron-density map. The experimental map derived from xenon MIR phases is readily interpretable even before density modification (Fig. 3*a*) and is as clear as that obtained from selenomethionine MAD data (Fig. 4*a*). To provide an objective comparison of map quality, real-space correlation coefficients were computed between experimental maps and maps calculated from refined atomic models at a resolution of 1.9 Å. For the map obtained from xenon derivatives, the correlation coefficient was 0.53 before density modification. In comparison, the map calculated from the selenomethionine data gave a slightly higher correlation coefficient of 0.61. After application of the solvent-flattening procedure (Figs. 3*b* and 4*b*), the agreement between experimental and calculated maps increased to 0.80 and 0.74 for xenon- and selenomethionine-derived maps, respectively.

## 4. Discussion

Although the binding of xenon within protein cavities has been studied in the past (*e.g.* Schoenborn, 1965; Schoenborn *et al.*, 1965; Tilton *et al.*, 1984), crystallographic experiments on noble-gas complexes have become increasingly popular in the last decade. This resurgence can be attributed to the successful use of xenon as a heavy atom for isomorphous replacement

(Vitali *et al.*, 1991) and to the development of devices for exposing protein crystals to high pressures of noble gases, both at ambient temperature (Schiltz *et al.*, 1994; Stowell *et al.*, 1996) and prior to freezing (Sauer *et al.*, 1997; Soltis *et al.*, 1997; Djinovic Carugo *et al.*, 1998; Machius *et al.*, 1999). Many of these devices are now commercially available (Xenon Chamber from Hampton Research, Cryo-Xe-Siter from Molecular Structures Corporation and Xcell from Oxford Cryosystems). In addition, anomalous dispersion data have been collected at the *K* edges of krypton ($\lambda = 0.86$ Å; Schiltz, Shepard *et al.*, 1997; Cohen *et al.*, 2001) and xenon ($\lambda = 0.36$ Å; Schiltz, Kvick *et al.*, 1997), adding to the potential of noble-gas complexes as sources of crystallographic phase information. Advantages of noble-gas complexes over traditional heavy-atom derivatives include the high degree of isomorphism with native crystals and the gentle conditions required for complex formation, both of which are the result of the comparatively weak van der Waals forces that stabilize bound noble-gas atoms.

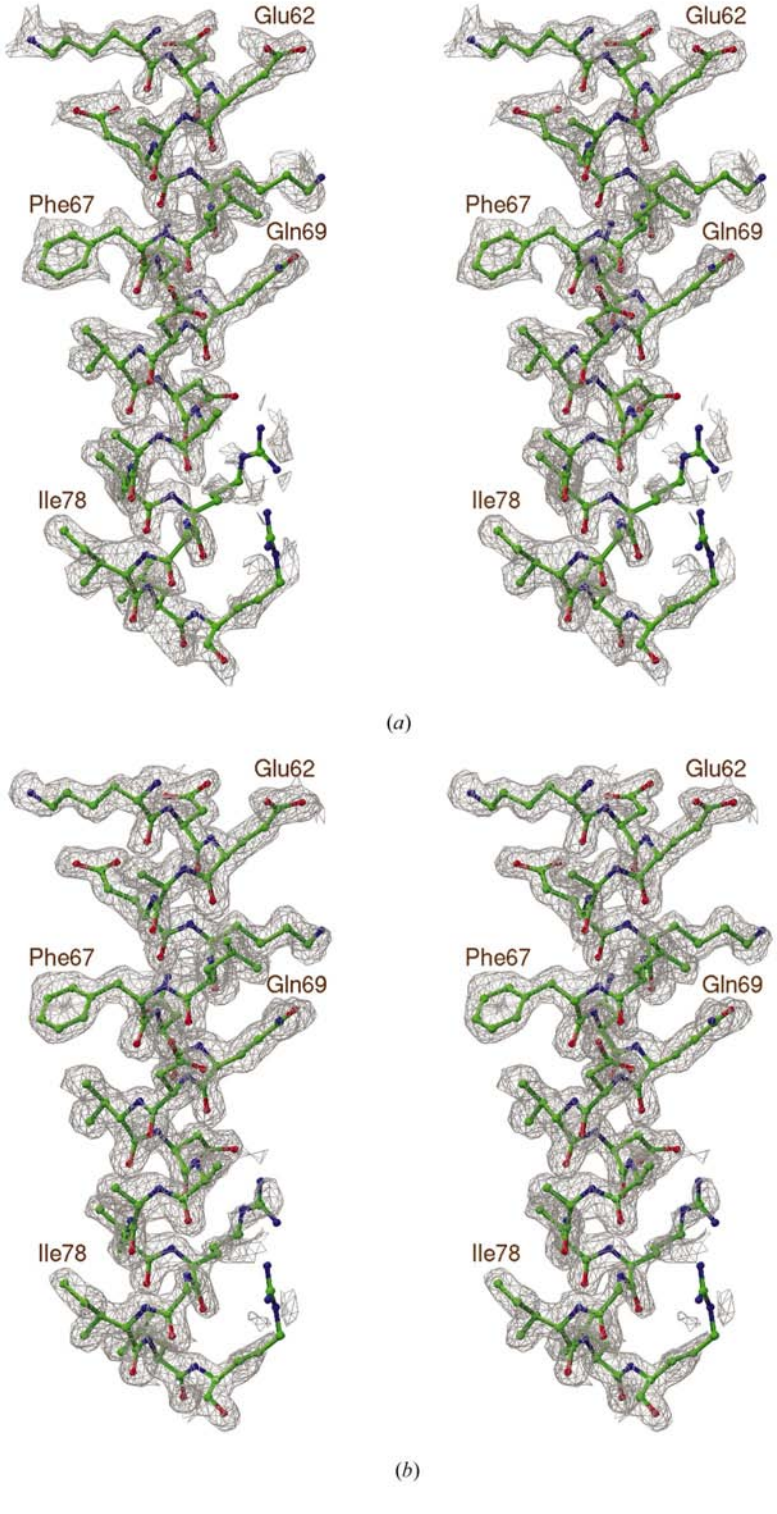


**Figure 4**
Stereoviews of representative electron density calculated using experimental phases from selenomethionine-containing L99A lysozyme (*a*) before and (*b*) after solvent flattening. The maps, which are at 1.6 Å resolution and contoured at 1.0$\sigma$, depict the central helix (residues 60–80). Refined coordinates for selenomethionine-containing L99A lysozyme are also shown.

The power of noble gases as a vehicle for *de novo* structure determination has been tempered by the realisation that not all proteins contain noble-gas binding sites. Only half are expected to contain cavities sufficiently large to bind noble gases (Stowell *et al.*, 1996). Furthermore, even in proteins which do bind noble gases, the resulting complex yields only a single derivative. While this derivative may be sufficient for multiwavelength anomalous dispersion (MAD) phasing, in the absence of additional derivatives crystallographers without access to tunable synchrotron sources will be limited to less powerful single isomorphous replacement with anomalous dispersion (SIRAS) techniques. In the course of an investigation into the nature of the forces which govern ligand binding within proteins (Quillin *et al.*, 2000), we found that by mutating large apolar residues to alanine, noble-gas binding sites in addition to the single site present in the wild-type protein could be introduced into T4 lysozyme. The potential of this approach for providing crystallographic phase information is illustrated by the results presented here.

Site-directed mutagenesis has proven to be a powerful tool for the determination of protein crystal structures (for a review, see Price & Nagai, 1995). Both cysteine (Sun *et al.*, 1987; Hatfull *et al.*, 1989; Nagai *et al.*, 1990; Martinez *et al.*, 1993) and methionine (Leahy *et al.*, 1994; Gassner & Matthews, 1999) residues have been introduced into proteins using this technique in successful attempts to generate novel heavy-atom derivatives. In another case, a cysteine residue was mutated to serine in order to improve isomorphism (Cook *et al.*, 1992). The

**Table 2**
Refined heavy-atom positions, $B$ factors and occupancies ($Q$) for xenon and selenomethionine derivatives.

| | | | | WT* | | L99A | | F153A | | L99A/F153A | |
|---|---|---|---|---|---|---|---|---|---|---|---|
| Atom | $x$ | $y$ | $z$ | $B$ (Å$^2$) | $Q$ | $B$ (Å$^2$) | $Q$ | $B$ (Å$^2$) | $Q$ | $B$ (Å$^2$) | $Q$ |
| Xe1 | 0.5386 | 0.1658 | 0.0063 | 13 | 0.47 | 19 | 0.49 | 13 | 0.44 | 14 | 0.47 |
| Xe2 | 0.4750 | 0.0981 | 0.0447 | — | — | 20 | 0.52 | — | — | 14 | 0.50 |
| Xe3 | 0.5084 | 0.1244 | 0.0233 | — | — | 74 | 0.10 | — | — | — | — |
| Xe4 | 0.5612 | 0.1123 | 0.0141 | — | — | — | — | 6 | 0.14 | 26 | 0.22 |
| Xe5 | 0.5769 | 0.0891 | −0.0426 | — | — | — | — | — | — | 5 | 0.06 |
| Se1 | 0.7502 | 0.0265 | 0.0803 | — | — | 49 | 1.00 | — | — | — | — |
| Se2 | 0.6785 | 0.0890 | 0.0703 | — | — | 34 | 1.00 | — | — | — | — |
| Se3 | 0.6077 | 0.1896 | 0.0216 | — | — | 11 | 1.00 | — | — | — | — |
| Se4 | 0.6460 | 0.2939 | 0.0421 | — | — | 24 | 1.00 | — | — | — | — |
| Se5 | 0.4980 | 0.1485 | −0.0928 | — | — | 19 | 1.00 | — | — | — | — |

**Table 3**
Phasing statistics for xenon and selenomethionine derivatives, calculated to 1.9 Å resolution.

| | | Phasing power | | | Figure of merit | |
|---|---|---|---|---|---|---|
| | | | Acentric | | | |
| Protein | Derivative | Centric | Iso | Ano | After *SHARP* | After *SOLOMON* |
| WT* | 0.8 MPa Xe | 1.38 | 2.25 | 1.24 | | |
| L99A | 0.8 MPa Xe | 1.32 | 1.95 | 1.42 | | |
| F153A | 0.8 MPa Xe | 1.14 | 1.57 | 0.94 | | |
| L99A/F153A | 0.8 MPa Xe | 1.37 | 1.81 | 1.43 | | |
| | | | | | 0.56 | 0.91 |
| L99A SeMet | Low | 0.00 | 0.00 | 1.06 | | |
| | Inflection | 1.51 | 2.90 | 4.88 | | |
| | Peak | 1.22 | 2.10 | 5.31 | | |
| | High | 0.28 | 0.34 | 4.46 | | |
| | | | | | 0.79 | 0.95 |

use of site-directed mutagenesis to create noble-gas binding sites for phase determination is the latest example of the potential of protein engineering to facilitate the determination of protein structures by X-ray crystallography.

A question which arises during application of this method concerns the choice of sites of mutation. Ideally, these sites would be located within the core of the protein for two reasons. Firstly, this ensures that an apolar cavity suitable for noble-gas binding is generated. Secondly, choosing sites far from crystal contacts simplifies crystallization and improves isomorphism. In the absence of a crystal structure, it is not obvious which residues are exposed and which are buried. Nevertheless, by selecting large apolar residues as sites of mutations, the probability of obtaining a suitable binding site is maximized, as the majority of these residues are completely buried (Rose *et al.*, 1985). Because of the potential for polar interactions, however, tyrosine and tryptophan residues should be avoided. In addition, because of the linear configuration of methionine, substitution of this residue may not yield cavities of sufficient width to bind the relatively large noble gases. This leaves leucine and phenylalanine as preferred residues for mutation. A rough estimate of the likelihood of success in generating noble-gas binding sites in a protein of unknown structure can be obtained from experience with T4 lysozyme. This protein contains 16 leucines, most of which have been replaced with alanine (Eriksson *et al.*, 1992; Xu *et al.*, 1998). In five cases interior cavities were created and in the three examples tested (L99A, L121A and L133A; Quillin *et al.*, 2000) noble gases bound within the cavity. Experience to date suggests that it is rare for a large-to-small substitution at an internal site not to result in the formation of a cavity (Xu *et al.*, 1998). In the case of L121A, the protein structure surrounding the site of the mutation collapses, but it still leaves a xenon-binding site between the 'wild-type' site and the site previously occupied by the side chain of Leu121 (Quillin *et al.*, 2000). This suggests that if leucine-to-alanine substitutions are made at random there is about a 30% chance of generating a useful noble-gas binding site. As well as the 16 leucines, there are five phenylalanines, ten isoleucines and nine valines in T4 lysozyme. Among these 24 additional bulky hydrophobic residues, substitution with alanine generates an internal cavity in seven cases (again, a success rate of about 30%). Except for F153A, however (Quillin *et al.*, 2000), it has not been determined whether the resultant cavities (Xu *et al.*, 1998) are large enough to bind noble gases.

In comparing the phasing statistics shown in Table 3, it should be kept in mind that each of the xenon derivatives includes the site that is present in the native protein. As judged by the heights of the Patterson peaks (Fig. 1) and the relative occupancies (Table 2) the 'non-native' xenon-binding sites in the L99A and L99A/F153A mutants contribute substantially to the phase determination, although the contribution in the case of F153A would appear to be less.

One caveat of using 'large-to-small' mutants for phasing is that the resulting protein may be destabilized owing to cavity formation. In T4 lysozyme, the loss of stability resulting from Leu→Ala mutations ranges from 11.3 to 20.9 kJ mol$^{-1}$ (Eriksson *et al.*, 1992, 1993; Xu *et al.*, 1998). Nevertheless, even in this relatively small protein, expression levels are sufficiently high that the loss of stability is not a cause of concern. Indeed the expression levels for mutant proteins grown in rich media are typically much higher than those obtained for wild-type proteins grown in minimal media during selenomethionine incorporation. In larger proteins, the destabilization that results from a single 'large-to-small' substitution may have less of an impact on protein expression owing to the larger size of the hydrophobic core.

With the current emphasis on high-throughput crystallography, methods for determining phases which are more reliable and less disruptive than traditional heavy-atom soaks are becoming increasingly important. The technique described in this paper will extend the utility of noble gases in this regard. It is of general applicability, including cases where selenomethionine incorporation may not be possible. It also allows the possibility of generating a series of distinct heavy-

atom derivatives. Finally, since each noble-gas binding site results from a defined substitution in the polypeptide chain, the knowledge of these sites will assist in the interpretation of the resultant electron-density map.

We thank Thomas Earnest and the staff of the Macromolecular Crystallography Facility at the Advanced Light Source for help with synchrotron data collection. The Advanced Light Source is supported by the Director, Office of Science, Office of Basic Energy Sciences, Materials Sciences Division of the US Department of Energy under Contract No. DE-AC03-76SF00098 at Lawrence Berkeley National Laboratory. MLQ acknowledges the support of a fellowship from the Helen Hay Whitney Foundation. This work was also supported in part by NIH grant GM20066 to BWM.

## References

Abrahams, J. P. & Leslie, A. G. W. (1996). *Acta Cryst.* D**52**, 30–42.
Bellizzi, J. J., Widom, J., Kemp, C. W. & Clardy, J. (1999). *Structure*, **7**, R263–R267.
Chen, W. & Bahl, O. P. (1991). *J. Biol. Chem.* **266**, 8192–8197.
Cohen, A., Ellis, P., Kresge, N. & Soltis, S. M. (2001). *Acta Cryst.* D**57**, 233–238.
Collaborative Computational Project (1994). *Acta Cryst.* D**50**, 760–763.
Cook, W. J., Jeffrey, L. C., Sullivan, M. L. & Vierstra, R. D. (1992). *J. Biol. Chem.* **267**, 15116–15121.
Dao-Pin, S., Alber, T., Bell, J. A., Weaver, L. H. & Matthews, B. W. (1987). *Protein Eng.* **1**, 115–123.
Dauter, Z. & Dauter, M. (2001). *Structure*, **9**, R21–R26.
Dauter, Z., Li, M. & Wlodawer, A. (2001). *Acta Cryst.* D**57**, 239–249.
Djinovic Carugo, K., Everitt, P. & Tucker, P. A. (1998). *J. Appl. Cryst.* **31**, 812–814.
Doublie, S. (1997). *Methods Enzymol.* **276**, 523–530.
Eriksson, A. E., Baase, W. A. & Matthews, B. W. (1993). *J. Mol. Biol.* **229**, 747–769.
Eriksson, A. E., Baase, W. A., Zhang, X. J., Heinz, D. W., Blaber, M., Baldwin, E. P. & Matthews, B. W. (1992). *Science*, **255**, 178–183.
Gassner, N. C., Baase, W. A., Hausrath, A. C. & Matthews, B. W. (1999). *J. Mol. Biol.* 294, 17–20.
Gassner, N. C. & Matthews, B. W. (1999). *Acta Cryst.* D**55**, 1967–1970.
Hatfull, G. F., Sanderson, M. R., Freemont, P. S., Raccuia, P. R., Grindley, N. D. & Steitz, T. A. (1989). *J. Mol. Biol.* **208**, 661–667.
Hendrickson, W. A., Horton, J. R. & LeMaster, D. M. (1990). *EMBO J.* **9**, 1665–1672.
Hendrickson, W. A. & Ogata, C. M. (1997). *Methods Enzymol.* **276**, 494–523.
La Fortelle, E. de & Bricogne, G. (1997). *Methods Enzymol.* **276**, 472–494.
Leahy, D. J., Erickson, H. P., Aukhil, I., Joshi, P. & Hendrickson, W. A. (1994). *Proteins*, **19**, 48–54.
Lustbader, J. W., Wu, H., Birken, S., Pollak, S., Gawinowicz Kolks, M. A., Pound, A. M., Austen, D., Hendrickson, W. A. & Canfield, R. E. (1995). *Endocrinology*, **136**, 640–650.
Machius, M., Henry, L., Palnitkar, M. & Deisenhofer, J. (1999). *Proc. Natl Acad. Sci. USA*, **96**, 11717–11722.
McWhirter, S. M., Pullen, S. S., Holton, J. M., Crute, J. J., Kehry, M. R. & Alber, T. (1999). *Proc. Natl Acad. Sci. USA*, **96**, 8408–8413.
Martinez, C., de Geus, P., Stanssens, P., Lauwereys, M. & Cambillau, C. (1993). *Protein Eng.* **6**, 157–165.
Matsumura, M. & Matthews, B. W. (1989). *Science*, **243**, 792–794.
Nagai, K., Oubridge, C., Jessen, T. H., Li, J. & Evans, P. R. (1990). *Nature (London)*, **348**, 515–520.
Otwinowski, Z. & Minor, W. (1997). *Methods Enzymol.* **276**, 307–326.
Price, S. R. & Nagai, K. (1995). *Curr. Opin. Biotechnol.* **6**, 425–430.
Quillin, M. L., Breyer, W. A., Griswold, I. J. & Matthews, B. W. (2000). *J. Mol. Biol.* **302**, 955–977.
Rose, G. D., Geselowitz, A. R., Lesser, G. J., Lee, R. H. & Zehfus, M. H. (1985). *Science*, **229**, 834–838.
Sauer, O., Schmidt, A. & Kratky, C. (1997). *J. Appl. Cryst.* **30**, 476.
Schiltz, M., Kvick, A., Svensson, O. S., Shepard, W., de La Fortelle, E., Prangé, T., Kahn, R., Bricogne, G. & Fourme, R. (1997). *J. Synchrotron Rad.* **4**, 287–297.
Schiltz, M., Prangé, T. & Fourme, R. (1994). *J. Appl. Cryst.* **27**, 950–960.
Schiltz, M., Shepard, W., Fourme, R., Prangé, T., de La Fortelle, E. & Bricogne, G. (1997). *Acta Cryst.* D**53**, 78–92.
Schoenborn, B. P. (1965). *Nature (London)*, **208**, 760–762.
Schoenborn, B. P., Watson, H. C. & Kendrew, J. C. (1965). *Nature (London)*, **207**, 28–30.
Sharff, A. J., Koronakis, E., Luisi, B. & Koronakis, V. (2000). *Acta Cryst.* D**56**, 785–788.
Smith, J. L. & Thompson, A. (1998). *Structure*, **6**, 815–819.
Soltis, S. M., Stowell, M. H. B., Wiener, M. C., Phillips, G. N. Jr & Rees, D. C. (1997). *J. Appl. Cryst.* **30**, 190–194.
Stowell, M. H. B., Soltis, S. M., Kisker, C., Peters, J. W., Schindelin, H., Rees, D. C., Cascio, D., Beamer, L., Hart, P. J., Wiener, M. C. & Whitby, F. G. (1996). *J. Appl. Cryst.* **29**, 608–613.
Sun, D. P., Alber, T., Bell, J. A., Weaver, L. H. & Matthews, B. W. (1987). *Protein Eng.* **1**, 115–123.
Tilton, R. F. Jr, Kuntz, I. D. Jr & Petsko, G. A. (1984). *Biochemistry*, **23**, 2849–2857.
Vitali, J., Robbins, A. H., Almo, S. C. & Tilton, R. F. (1991). *J. Appl. Cryst.* **24**, 931–935.
Xu, J., Baase, W. A., Baldwin, E. & Matthews, B. W. (1998). *Protein Sci.* **7**, 158–177.